



ORIGINAL ARTICLE

Eco-benign biodiesel production from waste cooking oil using eggshell derived MM-CaO catalyst and condition optimization using RSM approach



F. Nadeem^a, I.A. Bhatti^a, A. Ashar^{a,b,*}, M. Yousaf^a, M. Iqbal^{c,*}, M. Mohsin^a, J. Nisar^d, N. Tamam^{e,*}, N. Alwadai^e

^a Department of Chemistry, University of Agriculture, Faisalabad, Pakistan

^b Department of Chemistry, Govt. College Women University, Faisalabad, Pakistan

^c Department of Chemistry, The University of Lahore, Lahore, Pakistan

^d National Centre of Excellence in Physical Chemistry, University of Peshawar, Peshawar 25120, Pakistan

^e Department of Physics, College of Sciences, Princess Nourah bint Abdulrahman University (PNU), Riyadh 11671, Saudi Arabia

Received 20 April 2021; accepted 10 June 2021

Available online 15 June 2021

KEYWORDS

Heterogeneous catalyst;
Waste cooking oil;
Eggshells;
Biodiesel properties

Abstract Fatty acid methyl ester (FAME) was produced from waste cooking oil (WCO) utilizing eggshells derived solid base catalyst. Eggshells derived multi modal CaO (MM-CaO) also provides a cost-effective way for the preparation of green fuel. The nano-scaled MM-CaO was prepared using ball milling followed by calcination at 800 °C for 2 h from eggshells powder. The characterization of calcined powder was executed by XRD, EDX, SEM and FTIR techniques. Diffractogram of MM-CaO showed cubic crystal structure and presence of calcium, carbon and oxygen was confirmed by EDX. The morphology of MM-CaO was revealed by SEM having bandgap energy (3.02 eV) which declared MM-CaO as photoactive in solar range. Catalytic transesterification process furnished 75.2% yield, whereas in photocatalytic process, 86.8% yield was obtained at optimum conditions (temperature 50 °C, reaction time 180 min and 1.5 g catalyst dose). The FAME formation was monitored by GC and FTIR analysis. Physiochemical properties of produced biodiesel were also determined and equated with standards. Results depicted that MM-CaO is highly efficient for conversion of WCO to biodiesel.

© 2021 The Author(s). Published by Elsevier B.V. on behalf of King Saud University. This is an open access article under the CC BY-NC-ND license (<http://creativecommons.org/licenses/by-nc-nd/4.0/>).

* Corresponding author.

E-mail addresses: ambreenashar2013@gmail.com (A. Ashar), Bosalvee@yahoo.com (M. Iqbal), Nmtamam@pnu.edu.sa (N. Tamam).

Peer review under responsibility of King Saud University.



1. Introduction

Energy is one of the basic requirements in different sectors of life. As a viable fuel, oil has been serving the world to address its issue of energy utilization. Larger part of energy consumed is based on fossil fuel resources, which that are non-renewable. The reliance of mankind totally on the conventional fuels

could cause considerable deficiency in future. The energy demand is increased drastically, which on the other hand pollutes the environment by generating gases. The extensive use of fossil fuel is depleting its reserve and emitting a high concentration of air pollutants (Jafarnejad, 2016, 2017a,b; Jiménez-Cruz et al., 2021; Kuniyil et al., 2021; Tamborini et al., 2019). Renewable energy resources are efficient to substitute the conventional fossil-based fuels. Biodiesel is fatty acid methyl ester (FAME), a biomass-inferred fuel and it is an alternate to diesel fuel. It is free from or it contains very less aromatic content, low sulfur and low particulates content in diesel exhaust (Nisar et al., 2018). Biodiesel is eco-benign, easily transportable, readily accessible, safe and biodegradable (Atadashi et al., 2010; Mumtaz et al., 2017; Obi et al., 2020). Thus, the utilization of biodiesel is beneficial because of its natural cordiality over conventional diesel (Gangadhara and Prasad, 2016; Mootabadi et al., 2010; Ramos et al., 2019). A detail review related to biodiesel production based on various sustainable resources and systems has been documented by Ramos et al. (2019). Transesterification is an excellent process to produce biodiesel. Non-edible vegetable oil is the most effective feedstock for biodiesel because of its low cost (Fukuda et al., 2001; Hiwot, 2017; Mardhiah et al., 2017). In the transesterification process, both homogenous or heterogeneous catalysts can be utilized to enhance the rate of reaction (Sharma and Rangaiah, 2013). However, the use of homogeneous catalyst KOH/NaOH is not preferable because it is difficult to handle in reaction mixture, like separation and purification etc. Heterogeneous catalysis has supremacy to thrash the harms of homogeneous catalysis (Hiwot, 2018; Pedavoah et al., 2018). The solid catalysts can be used, separated and reutilize because of their easy separation (Huang et al., 2013). CaO catalyst can be prepared from different waste sources, i.e., eggshells containing 94% CaCO₃ (Pedavoah et al., 2018). The CaCO₃ constituent can be transformed into CaO and CO₂ under elevated temperature (Jazie et al., 2013; Kesić et al., 2016). CaO is also known as quick lime or burnt lime (Joya et al., 2016). Amongst the heterogeneous impetuses that are utilized in transesterification, CaO has a prominent position (Kostić et al., 2016; Niju et al., 2014; Puna et al., 2010). The oil reacts with methanol in the existence of a catalyst and forms esterified vegetable oil by a process called transesterification (Ranganathan and Sampath, 2011).

The CaO is a semiconductor. It consisting of Ca(OH)₂, CaCO₃ and CaO so-known as multi-model CaO (MM-CaO). It can be employed as an efficient heterogeneous catalyst due to its promising catalytic activity (Song and Zhang, 2010). In the presence of sunlight, the efficiency of MM-CaO increased and it has been used in the formation of biodiesel. When sunlight falls on the surface of MM-CaO electrons of the VB get excited and due to excess energy, these electrons move from VB to CB and generate electron-hole pairs ($\text{CaO} + h\nu \rightarrow h^+ + e^-$) and participate in a chemical reaction. The generated hole attack on methanol adsorbed on the catalyst surface and form H⁺ and CH³O[•]. Methanol is oxidized by +ve hole. At the same time R-COOH[•] form by the reduction of RCOO-H adsorbed on the catalyst surface reacting with photo-generated electron. The produced CH₃O[•], H⁺, RCOO-H[•] then react to form intermediates and finally, the transesterification process occurred (Corro et al., 2013).

Present study was carried out to prepare biodiesel from WCO through using catalytic process. MM-CaO was used as

an efficient heterogeneous photocatalyst derived from waste eggshells. Catalytic and photocatalytic transesterification processes were employed to compare the enhancement in biodiesel yield. Optimization of variables like reaction parameters was done by response surface methodology.

2. Material and methods

2.1. Material and reagents

Waste vegetable oil and eggshells were obtained from the local restaurant, Faisalabad, Pakistan. NaOH/KOH, HCl acid and CH₃OH were procured from sigma Aldrich and distilled water is used for the preparation of solutions and washing purposes throughout the study.

2.2. Treatment of waste oil and preparation of MM-CaO

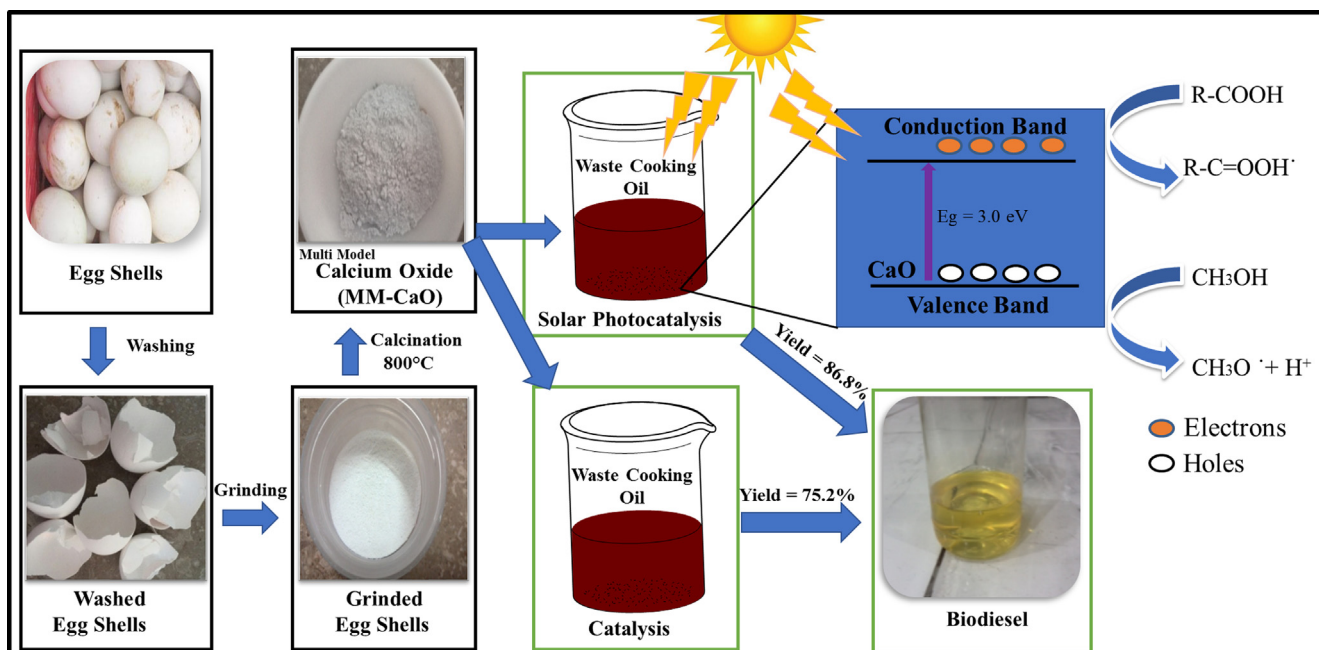
Waste vegetable oil contains many food residues and also water, which increased the free fatty acid value i.e., 2.5% of waste oil that resulted in the formation of large amount of soap instead of biodiesel. Therefore, it needed treatment before its use. Food residues from WCO were eliminated by filtration and after filtration oil was heated to remove water. MM-CaO was prepared from eggshells, which were washed with excess water in order to eradicate impurities on its surface and then dried at room temperature and after drying, ground in a ball mill to fine powder followed by calcination (Muffle Furnace) at 800 °C for 2 h in order to transform CaCO₃ content of eggshells into MM-CaO (Scheme 1 and Fig. 1).

2.3. Transesterification

Transesterification process was done to transform the oil into biodiesel. Photocatalytic transesterification was done in the occurrence of natural sunlight and a hot plate was utilized as an external heating source and a thermometer was also utilized in order to maintain the required reaction temperature. MM-CaO was mixed in methanol by stirring for 45 min and then WCO was heated below the boiling point of methanol i.e., 64.5 °C and after this methanol, MM-CaO mixture was added in by 3:1 oil to methanol molar ratio. The contents were agitated for 30 min and irradiated to sunlight. After reaction completion, the product was allowed to settle for one day for complete separation of layers. The reaction was done at different catalyst doses, reaction temperature and irradiation time in order to determine maximum yield. Catalytic transesterification was also done under the similar optimized conditions but in the absence of light.

2.4. Characterization of MM-CaO

X-ray diffraction (XRD, JoelJDX-3532 diffractometer, Japan) analysis was performed out to deduce the crystal structure. Particle size was determined by the Debye formula. Scanning Electron Microscopy (SEM, Quanta 250, FEG (USA) analysis was conducted to determine the surface morphology. The EDX analysis was done to identify the elements present in the prepared material. Fourier transform infrared spectroscopy (FTIR, Bruker IFS 125HR Japan) was done to identify the functional groups.



Scheme 1 Representation of MM-CaO synthesis and biodiesel production application.

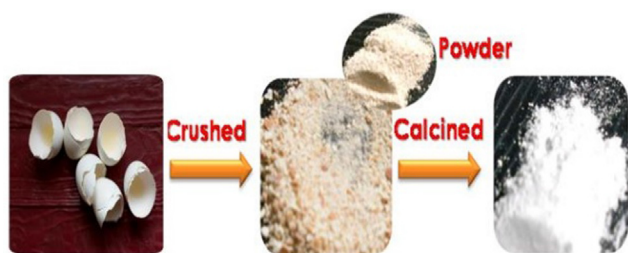


Fig. 1 Schematic presentation for the preparation of MM-CaO.

2.5. Statistical analysis

A three-level factorial, central composite design (CCD) was applied for the optimization of conditions by utilizing designer expert (version 7.0.0) (Zhang et al., 2011). The RSM utilizing CCD was utilized (Kirubakaran and Selvan, 2021) to optimize

the operational reaction parameters (i.e., catalyst dose, temperature and reaction irradiation time). A complete design for photocatalytic and catalytic processes are depicted in Tables 1 and 2.

2.6. Analysis of biodiesel (FAME)

FTIR of biodiesel was done to determine the functional groups. GC analysis of biodiesel was done to identify FAME and conditions are given in Table 3.

2.7. Biodiesel properties

Flash and fire point of biodiesel was calculated by utilizing an open cup tester. Iodine value (IV) was determined by taking 0.1 g biodiesel sample in a 250 mL iodine flask and mixed in 20 mL CCl_4 and wijs solution (25 mL), which was placed for 30 min in dark and KI solution (20 mL) and water (100 mL)

Table 1 Process variables at three levels employed for photocatalytic process.

Factors	Variables	Units	Lower-Level	Higher-Level
A	Photocatalyst concentration	g	0.5	2.5
B	Temperature	°C	34	66
C	Sunlight Irradiation Time	Minutes	120	240

Table 2 Process variables and their levels employed in CCD for catalytic process.

Factors	Variables	Units	Lower-Level	Higher-Level
A	Catalyst concentration	g	0.50	2.5
B	Temperature	°C	34	66
C	Time	Minutes	120	240

Table 3 GC conditions for FAME analysis.

Column	DBWEX 30 M 0.25
Mobile phase	Nitrogen
Flow rate	30 mL/min
Split flow	51 mL
Injection	0.49 μ l
Volume	
Detection	FID (260 $^{\circ}$ C)
FID	140 $^{\circ}$ C for 2 min to 250 $^{\circ}$ C @ 2.3/min, injector
Temperature	240 $^{\circ}$ C

was mixed in it. The contents thus obtained was titrated (using 0.1N $\text{Na}_2\text{S}_2\text{O}_3 \cdot 5\text{H}_2\text{O}$) in the presence of indicator (starch solution).

$$IV = \frac{\text{Blank} - \text{sample.NNa}_2\text{S}_2\text{O}_3.127.100}{\text{Sample mass(g)}} \quad (1)$$

For saponification value (SV) determination, biodiesel (0.5 g) and KOH (alcoholic) solution (20 ml) was mixed, which was heated in a condenser till a clear solution and after cooling (room temperature) the content, indicator (few drop of phenolphthalein) was dropped and

$$SV = \frac{\text{Blank} - \text{sample.N.56.1}}{\text{Sample mass(g)}} \quad (2)$$

Cetane number (CN) indicates the quality of biodiesel (Sivaramakrishnan and Ravikumar, 2012), which was assessed using a relation $\text{CN} = 46.3 + 5458/\text{SV} - 0.225 \cdot \text{IV}$.

For acid value (AV) determined, oil (0.5 g), ethanol (10 mL) along with indicator (2 drop, phenolphthalein) was taken in a flask and content was titrated using NaOH (0.1N) and end point was noted on the appearance of pink color. Free fatty acid (FFA) as oleic acid was calculated by this formula, $\text{FFA}\% = \text{V} \cdot \text{N} \cdot 28.2/\text{w}$. Where, v is the volume in ml of titrated solution, N is the normality, w is the sample mass in g, %age FFA was converted into AV by formula, $\text{AV} = 1.989 \cdot \text{FFA}\%$.

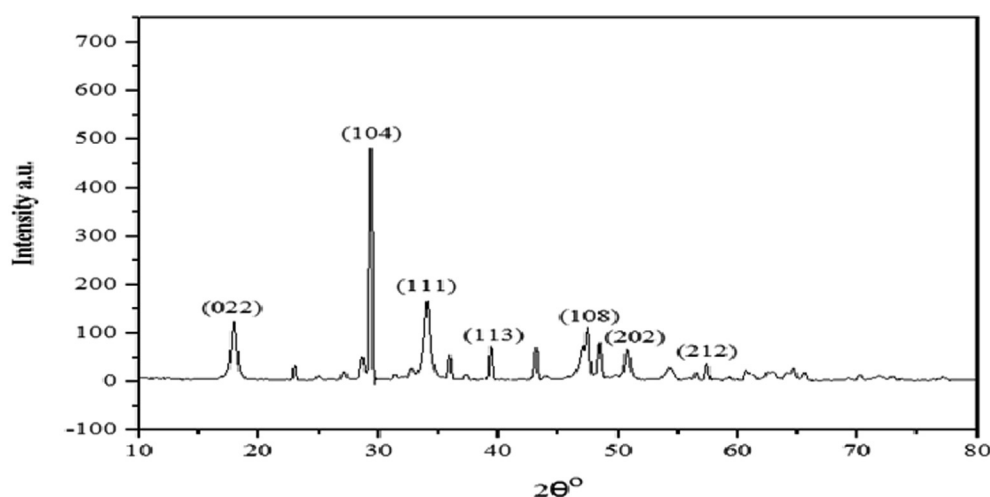
3. Results and discussion

3.1. Characterization

XRD analysis was performed (Amer and Awwad, 2021; Shammout and Awwad, 2021), to study the crystal structure (Fig. 2). The peaks recorded in diffractogram at 18.67° , 29.89° , 32.2 , 34.08° , 37.3 , 39.40° , 47.50° , 51.39° , 57.48° . The diffraction peak appeared at 29.89° was of CaCO_3 indicating the high concentration of calcite in the sample. Small diffraction peaks appeared at 2θ value of 32.2° , 37.39° , 47.50° , 51.3° , 57.48° were for MM-CaO, which were in good conformity with standard JCPDS file (JCPDS82-1691). Small diffraction peaks also appeared at 18.67° , 34.08° were for $\text{Ca}(\text{OH})_2$. XRD analysis results showed that CaO has cubic crystal structure, $\text{Ca}(\text{OH})_2$ with rhombohedral crystal and MM-CaO particle size was of 41 nm.

The FTIR of MM-CaO was done to identify the functional group involved (Al-Fa et al., 2021; Awwad et al., 2020b) and outcome is depicted in Fig. 3. The sharp peak appeared at 3640 cm^{-1} was due to the O—H group. The strong peak at 500 cm^{-1} indicated the existence of Ca—O bond. Peaks at 1410 cm^{-1} , 1180 cm^{-1} and 850 cm^{-1} were due to C—O bond related to the carbonation of CaO nano-particles (Jazie et al., 2012). The SEM analysis was done to determine the morphology of the prepared catalyst (Awwad and Amer, 2020; Awwad et al., 2020a) and outcomes are displayed in Fig. 4. At high magnification plate like structures are visible in micrographs. Due to high surface charge the plates are agglomerated and surface of plates is rough and porous (Lee et al., 2015).

EDX was done to identify the individual elements. EDX analysis confirmed that sample contained calcium, carbon, oxygen and traces of magnesium (Fig. 5). Outcomes also showed that calcium is present in large amount as compared to oxygen. EDX analysis of synthesized MM-CaO is shown in Table 4. Diffused reflectance spectroscopy (DRS) of MM-CaO was performed to find out the optical properties. In the presence of sunlight excitation of electron to conduction band

**Fig. 2** XRD analysis of MM-CaO.

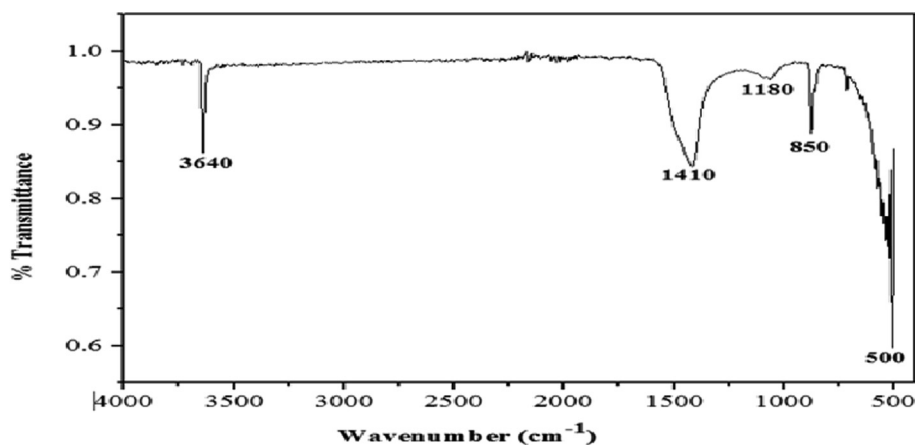


Fig. 3 FTIR analysis of MM-CaO.

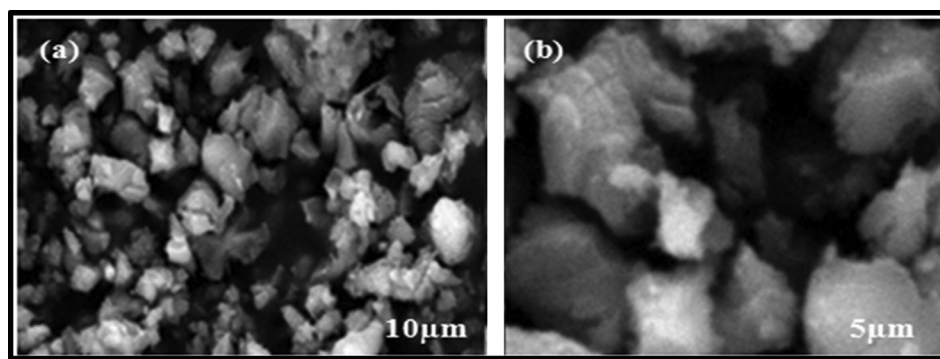


Fig. 4 SEM analysis of MM-CaO (a) at 5 K Magnification (b) at 25 K Magnification.

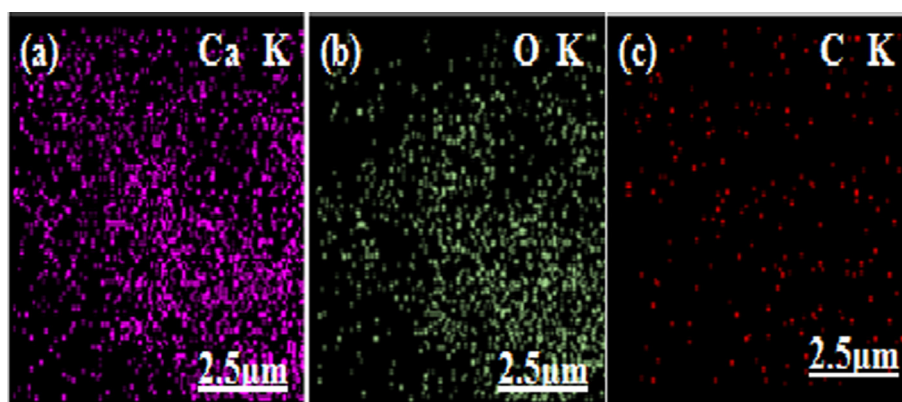


Fig. 5 EDX of MM-CaO, a) Surface concentration of calcium b) oxygen and c) carbon.

leads to generation of electron and hole pair. This can be attributed to band gap energy falling in the solar region (Fig. 6a). On inserting DRS data in Kubelka–Munk relationship, the band gap energy was calculated to be 3.02 eV (Fig. 6b). This value of band gap energy further supported that harvesting of solar radiation in the visible region was likely to carry out photocatalysis for synthesis of biodiesel.

3.2. Biodiesel synthesis and optimization

Synthesis of biodiesel was done by two routes, i.e., catalytic and photocatalytic transesterification process for biodiesel production. Optimization of independent variables, i.e., catalyst dose, temperature and sunlight irradiation time were studied. RSM in combination with CCD was utilized for

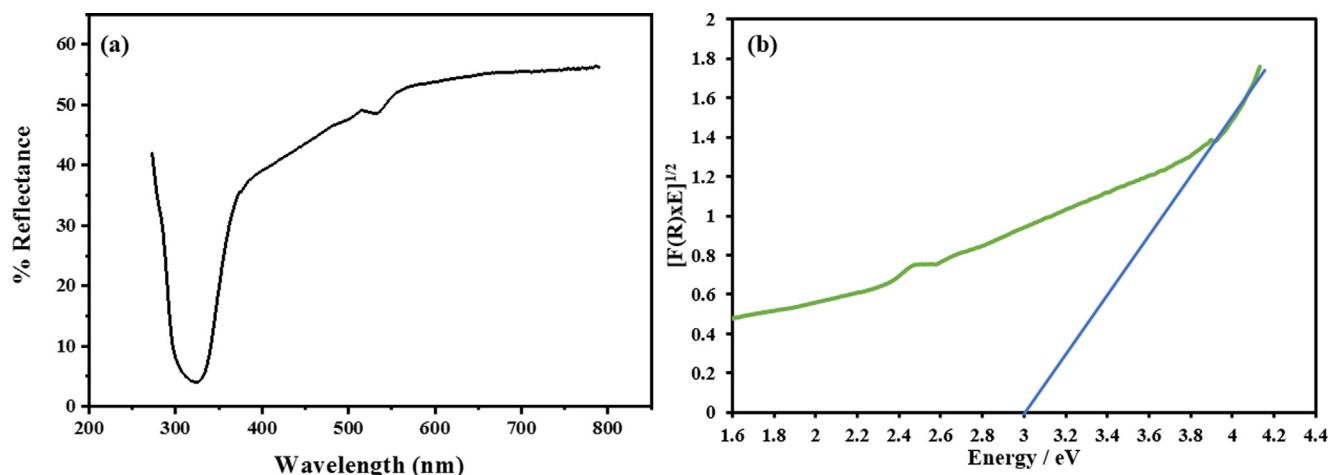
Table 4 EDX data of synthesized MM-CaO.

Sr No.	Element	Symbol	Mass%
1	Calcium	Ca	61.5
2	Oxygen	O ₂	24.4
3	Carbon	C	13.2
4	Magnesium	Mg	0.9

determining the interaction between the independent operational factors. The list of variables, their actual lower and higher levels for are given in the following [Tables 1 and 2](#). Design expert software utilized 3 factors CCD with 6 axial and 6 center points. The following term represents the total number of runs was carried as, ($2^3 = 8$) + ($2 \times 3 = 6$; axial points) + 6 (center points; 6 replication) = 20. Biodiesel yield was determined as (Yield% = Biodiesel weight/Weight of oil * 100).

3.3. Effect of process variables on biodiesel production

The ANOVA (analysis of variance) was done to find out the significance of the process variables and their interaction for biodiesel production ([Tables 5 and 6](#)). Model F-value of 104.00 specifies the significance of the developed model. Values of “Prob > F” lower than 0.0500 specify that model terms are significant and A, B, A², B², C² are found to be significant to enhance the biodiesel production. Values larger than 0.1000 points out that model terms are not considerable. The F-value (3.03) in Lack of Fit designates non-comparison with pure error and its chances are 12.39% of this higher value of Lack of Fit, which reveals the goodness of the model. Non-significant lack of fit is best. The Predicted R² of 0.9356 is in appropriate conformity with Adj R² of 0.9799. Adequate accuracy calculates the signal-to-noise ratio. A fraction larger than 4 is desirable. A ratio of 36.124 shows enough signal. Predicted value of R² = 0.9356 suggests that the information fit effectively with the design in the selected range ([Mohsin et al., 2020](#)).

**Fig. 6** (a) DRS of MM-CaO and (b) Band gap energy of MM-CaO.**Table 5** ANOVA performed for photocatalytic process for biodiesel production.

Source	Sum of squares	DF	Mean square	F-value	P-value	prob > F
Model	7780.71	9	864.52	104.0	< 0.0001	significant
A-Photocatalyst conc.	195.03	1	195.03	23.46	0.0007	
B-Temperature	1094.56	1	1094.56	131.67	< 0.0001	
C-Sunlight radiation time	39.26	1	39.26	4.72	0.0549	
AB	1.71	1	1.71	0.21	0.6597	
AC	9.90	1	9.90	1.19	0.3007	
BC	3.51	1	3.51	0.42	0.5304	
A ²	557.52	1	557.52	67.07	< 0.0001	
B ²	6184.36	1	6184.36	743.93	< 0.0001	
C ²	78.29	1	78.29	9.42	0.0119	
Residual	83.13	10	8.31			
Lack of Fit	62.52	5	12.50	3.03	0.1243	Insignificant
Pure Error	20.61	5	4.12			
Cor Total	7863.84	19				

Std. Dev. = 2.88 R² = 0.989 AdjR² = 0.9799 Estimated R² = 0.9356 Adequate precision = 36.12

C.V = 4.48%

Table 6 ANOVA performed for catalytic process for biodiesel production.

Source	Sum of squares	DF	Mean square	F-value	P-value	prob > F
Model	4661.86	9	517.98	104.0	< 0.0001	significant
A-Catalyst conc.	122.81	1	122.81	36.30	0.0001	
B-Temperature	4398.11	1	1398.11	1299.89	< 0.0001	
C-Time	80.13	1	80.13	23.68	0.0007	
AB	0.10	1	0.10	0.030	0.8661	
AC	0.031	1	0.031	9.236E-0030.9253		
BC	0.031	1	0.031	9.236E-003		
A ²	32.56	1	32.56	9.62	0.0112	
B ²	29.57	1	29.57	8.74	0.0144	
C ²	78.29	1	78.29	9.42	0.0119	
Residual	1.01	10	1.01	0.30	0.5968	
Lack of Fit	24.55	5	4.91	2.65	0.1546	Insignificant
Pure Error	9.28	5	1.86			
Cor Total	4695.76	19				

Std. Dev. = 1.84 $R^2 = 0.993$ $AdjR^2 = 0.9863$ Estimated $R^2 = 0.9575$ Adequate precision = 36.41
C.V = 3.89%

The F-value of 153.09 is also an indication of model significance and there may be 0.01% coincidence of larger F-value due to noise. The $P < 0.0500$ is also another criteria of model significance of the developed model and based on this criteria the A, B, C, A², B² terms are significant. The Predicted R^2 (0.9575) and adjusted R^2 (0.9863), model is also significant because these values are close to 1. Hence, based on Lack of Fit, P value and R values this model values provide the significance of the regression model applied to deduce the effect of input variables. It also shows the connection between response and independent operational variables. "Adequate Precision" determines the signal-to-noise ratio. A ratio larger than 4 is enviable. Fraction of 46.408 suggests a sufficient signal. Predicted $R^2 = 0.9928$ suggests that the data fit well with the model in the studied range. On the other hand, residual analysis was done to confirm the adequacy of the model. This was done by observing the normal possibility plot of the residuals. Results showed that the photocatalytic transesterification

process provided 86.8% yield of biodiesel. Biodiesel was also prepared by catalytic transesterification process utilizing catalyst dose 1.5 g, reaction time 180 min., temperature 50 °C. Catalytic process gives 75.2% yield that is approximately 10% less than the photocatalytic process, which is because in the presence of sunlight efficiency of MM-CaO was enhanced (Song and Zhang, 2010). Normal possibility residual plots of photocatalysis and catalysis are shown in Fig. 7. Almost >85% point existed on the standard line (Fig. 7) that confirmed the fitness of the model.

The interactive impact of catalyst dose and temperature is shown in Fig. 8(a). It can be apparently seen that a rise in temperature and catalyst dose leads to increase in biodiesel yield, but only up to a certain limit. This is because if the temperature is above the BP of methanol, it starts to evaporate, and large quantity of catalyst dose leads to soap formation instead of biodiesel due to its basic nature. Conclusively, 50 °C is the optimum temperature and 1.5 g is the optimum catalyst dose

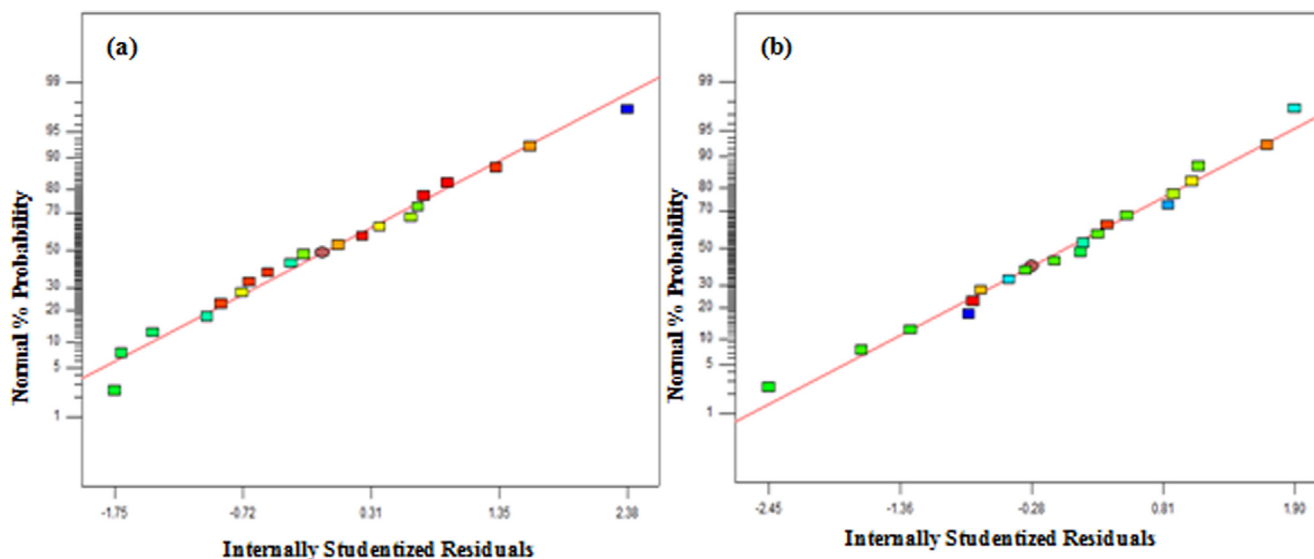


Fig. 7 Normal possibility plot of residuals for (a) photocatalytic and (b) catalytic processes.

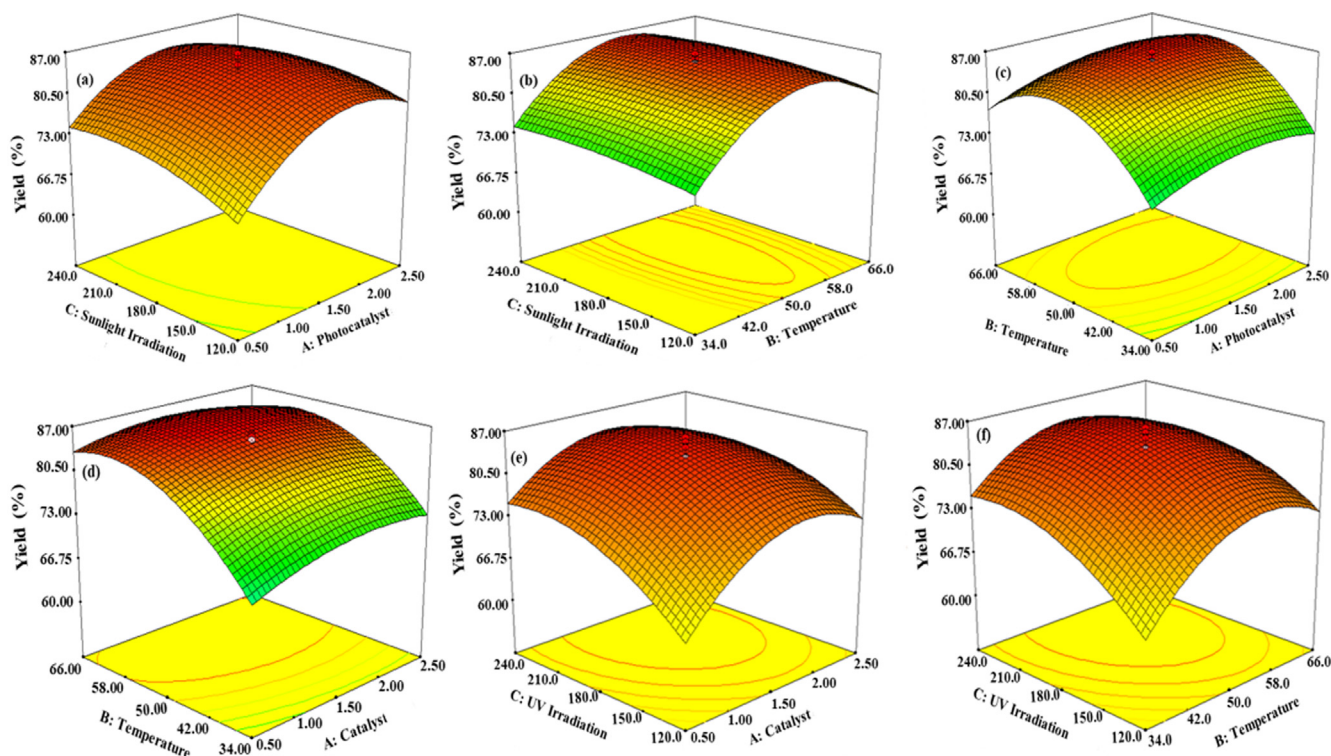


Fig. 8 3D plots of biodiesel yield as a function of (a) Sunlight Irradiation versus photocatalyst, (b) Sunlight Irradiation versus temperature, (c) temperature versus photocatalyst, (d) temperature versus catalyst, (e) UV irradiation and catalyst & (f) UV irradiation and temperature.

for maximum production of biodiesel. The input variables catalyst dose and time of irradiation impact on the yield is shown in Fig. 8(b). The irradiation time also affected the yield of biodiesel. It has been shown that as irradiation time has been increased methyl ester yield also increased, but only a certain limit, i.e., 180 min. The mutual effect of sunlight irradiation time and temperature for the production of biodiesel is shown in Fig. 8(c). The biodiesel production enhanced with irradiation time and temperature. But, at higher temperatures; the yield was decreased. Investigation showed that 50 °C is the optimum temperature (Nejad and Zahedi, 2018).

The interactive impact of catalyst and temperature on biodiesel production is seen in Fig. 8(d). It can be clearly observed that catalyst dose has positive impact on the amount of biodiesel, but higher amount did not affect the yield of biodiesel. A 1.5 g catalyst dose gives maximum quantity of biodiesel. The biodiesel yield was enhanced by increasing the temperature and catalyst dose up to certain limit. This is because if temperature increased above the boiling point of methanol, methanol starts to evaporate, and enormous dose of catalyst leads to the production of soap instead of biodiesel due to its basic nature. Hence, 50 °C is the optimum temperature (Onukwuli et al., 2017). The interactive impact of reaction time and catalyst dose on the yield of biodiesel is depicted in Fig. 8(e). A remarkable interaction among catalyst and reaction time on methyl ester yield was observed. Reaction time also affected the yield of biodiesel. The interactive effect of heating time and temperature on biodiesel yield is depicted in Fig. 8(f). Biodiesel yield increases with the increase in time and temperature. As heating

time increased methyl ester yield also increased, but after certain limit, a raise in time does not influence the yield of biodiesel. As the temperature increased, the yield was also enhanced up to 50 °C, which is the optimum level for maximum yield of biodiesel. The findings revealed the MM-CaO is highly efficient for the conversion of WCO to biodiesel and this process is economical versus other physico-chemical methods. The biodiesel thus produced will be used in combination to the diesel fuel, which will help to lessen the environmental issue of pollution (Abulude et al., 2018; Chokor, 2021; Mene and Iwuoha, 2021; Sasmaz, 2020; Sinanoglu and Sasmaz, 2019; Tsegaye et al., 2021).

3.4. Analysis of FAME

FTIR of analysis of FAME was done for the identification of functional groups (Al Banna et al., 2020). A band at 742 cm^{-1} was due to $=\text{C}-\text{H}$ groups, which indicates a methylene functional presence (Thanh et al., 2012). The characteristic peak found at 1185 cm^{-1} is attributed to $\text{O}-\text{CH}_3$, which is a typical of biodiesel (Fig. 9). The peak at 1410 cm^{-1} is correlated with $\text{C}-\text{H}$ methyl group. The peak at 1750 cm^{-1} is ascribed to $\text{C}=\text{O}$ groups, which indicate the presence of carbonyl functional groups in the biodiesel (Oyerinde and Bello, 2016). This group also revealed the transformation of triglycerides in the oil to methyl ester (Popovicheva et al., 2017; Saifuddin and Refal, 2014). The peaks at 2820 and 2940 (cm^{-1}) exhibited is due to of $\text{C}-\text{H}$ groups (symmetric/asymmetric), which indicating the presence of methyl or methylene group ($-\text{CH}_3$) in

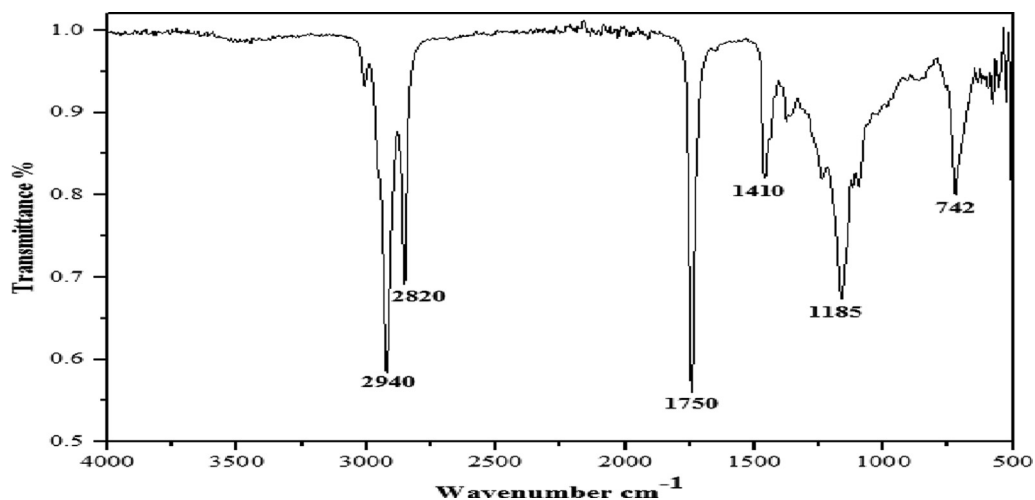


Fig. 9 FTIR analysis of biodiesel prepared using MM-CaO from waste cooking oil.

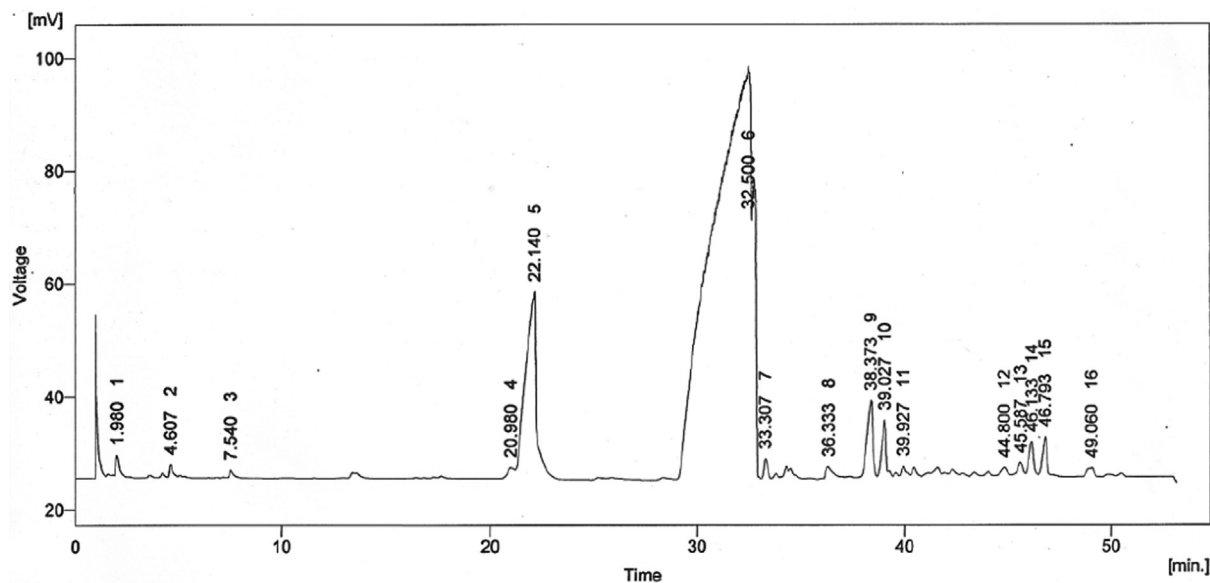


Fig. 10 GC analysis of prepared biodiesel utilizing MM-CaO from waste cooking oil.

Table 7 FAME composition of synthesized Biodiesel.

No.	Retention time	Conc. %	Identified compound
1	1.980	0.3	Butyric acid methyl ester (ME)
2	4.607	0.2	Enanthaic acid ME
3	7.540	0.1	Caprylic acid ME
4	20.980	0.4	Capric acid ME
5	22.140	9.7	Capric acid ME
6	32.500	78.4	Myristoleic acid ME
7	33.307	1.1	Myristic acid ME
8	36.333	0.6	Unknown
9	38.373	2.2	Penta decanoic acid ME
10	39.027	1.5	Heptadecanoic acid ME
11	39.927	1.9	Palmitoleic acid ME
12	45.587	0.14	α -Linoleic acid ME
13	46.793	1.0	γ -Linoleic acid ME
14	49.060	0.6	Nonadecanoic acid ME

biodiesel structure of ester. FAME was monitored using method reported elsewhere. FAME composition was identified by GC analysis (Farooq et al., 2015) (Fig. 10). The peaks that appeared in the chromatogram, correspond to different FAME present in the biodiesel sample. The composition of FAME determined by GC is shown in Table 7.

The properties of biodiesel like SV, IV, CN, AV, flash point, fire point, cloud & pour point was determined & then compared with standards (American Society for Testing Materials (ASTM D-6751), European Union Standard for biodiesel fuel (EN 14214)) reported and displayed in Table 8. IV determines the degree of un-saturation. CN determines the quality of biodiesel (Okullo et al., 2012). Flashpoint of biodiesel showed that it is a safer fuel due to its higher ignition temperature. The pour point of biodiesel revealed the temperature at which biodiesel becomes solid and no longer flows.

Table 8 Properties of Biodiesel in comparison with standards.

Properties	Unit	Prepared Biodiesel	ASTM-D6751	EN-14214
Saponification Value	mg KOH/g	242	–	–
Iodine value	mgI ₂ /g	59	–	max 110
Cetane number	55	47	48–60	–
Acid Value	mg KOH/g	0.87	< 0.7	< 0.5
Flashpoint	°C	135	100–170	120
Fire point	°C	150	100–170	–
Cloud point	°C	10	–3 to 12	–
Pour point	°C	4	–15 to 16	–

4. Conclusion

Biodiesel is an alternate and renewable energy fuel. Biodiesel was prepared by utilizing eggshells derived catalyst from WCO. The MM-CaO demonstrated an efficient and effective efficiency as catalyst for the transformation of WCO into biodiesel. Transesterification process was employed for the production of biodiesel. The catalytic and photocatalytic processes yielded 75.2 and 86.8 (%) biodiesel under optimized conditions, i.e., temperature 50 °C, reaction time 180 min and 1.5 g catalyst dose. Results showed that the photocatalytic transesterification process enhances the yield up to 11.6% as compared to catalytic process. Hence photocatalysis process shows more efficiency. Chemical properties of biodiesel were also determined in comparison to European and American standards, which were in the recommended limit. Based on efficiency, the catalyst derived from eggshell is economical and eco-benign, which could be used for the conversion of WCO into biodiesel.

Declaration of Competing Interest

The authors declare that they have no known competing financial interests or personal relationships that could have appeared to influence the work reported in this paper.

Acknowledgment

This research was funded by the Deanship of Scientific Research at Princess Nourah bint Abdulrahman University through the Fast-track Research Funding Program.

References

- Abulude, F.O., Ogunmola, D.N., Alabi, M.M., Abdulrasheed, Y., 2018. Atmospheric deposition: Effects on sculptures. *Chem. Int.* 4, 136–145.
- Al-Faouri, A.M., Abu-Kharma, M.H., Awwad, A.M., 2021. Green synthesis of copper oxide nanoparticles using Bougainvillea leaves aqueous extract and antibacterial activity evaluation. *Chem. Int.* 7, 155–162.
- Al Banna, L.S., Salem, N.M., Jaleel, G.A., Awwad, A.M., 2020. Green synthesis of sulfur nanoparticles using Rosmarinus officinalis leaves extract and nematocidal activity against Meloidogyne javanica. *Chem. Int.* 6, 137–143.
- Amer, M.W., Awwad, A.M., 2021. Green synthesis of copper nanoparticles by Citrus limon fruits extract, characterization and antibacterial activity. *Chem. Int.* 7, 1–8.
- Atadashi, I., Aroua, M., Aziz, A.A., 2010. High quality biodiesel and its diesel engine application: a review. *Renew. Sustain. Energy Rev.* 14, 1999–2008.
- Awwad, A.M., Amer, M.W., 2020. Biosynthesis of copper oxide nanoparticles using Ailanthus altissima leaf extract and antibacterial activity. *Chem. Int.* 6, 210–217.
- Awwad, A.M., Amer, M.W., Salem, N.M., Abdeen, A.O., 2020a. Green synthesis of zinc oxide nanoparticles (ZnO-NPs) using Ailanthus altissima fruit extracts and antibacterial activity. *Chem. Int.* 6, 151–159.
- Awwad, A.M., Salem, N.M., Aqarbeh, M.M., Abdulaziz, F.M., 2020b. Green synthesis, characterization of silver sulfide nanoparticles and antibacterial activity evaluation. *Chem. Int.* 6, 42–48.
- Chokor, A.A., 2021. Total petroleum and aliphatic hydrocarbons profile of the River Niger surface water at Okpu and Iyiowa-Odekpe regions in South-Eastern. Nigeria. *Chem. Int.* 7, 188–196.
- Corro, G., Pal, U., Tellez, N., 2013. Biodiesel production from Jatropha curcas crude oil using ZnO/SiO₂ photocatalyst for free fatty acids esterification. *Appl. Catal. B* 129, 39–47.
- Farooq, M., Ramli, A., Naeem, A., 2015. Biodiesel production from low FFA waste cooking oil using heterogeneous catalyst derived from chicken bones. *Renew. Energy* 76, 362–368.
- Fukuda, H., Kondo, A., Noda, H., 2001. Biodiesel fuel production by transesterification of oils. *J. Biosci. Bioeng.* 92 (5), 405–416.
- Gangadhara, R., Prasad, N., 2016. Studies on optimization of transesterification of certain oils to produce biodiesel. *Chem. Int.* 2, 59–69.
- Hiwot, T., 2017. Determination of oil and biodiesel content, physicochemical properties of the oil extracted from avocado seed (Persea Americana) grown in Wonago and Dilla (gedeo zone), southern Ethiopia. *Chem. Int.* 3, 311–319.
- Hiwot, T., 2018. Mango (Magnifera indica) seed oil grown in Dilla town as potential raw material for biodiesel production using NaOH-a homogeneous catalyst. *Chem. Int.* 4, 198–205.
- Huang, W., Tang, S., Zhao, H., Tian, S., 2013. Activation of commercial CaO for biodiesel production from rapeseed oil using a novel deep eutectic solvent. *Ind. Eng. Chem. Res.* 52 (34), 11943–11947.
- Jafarinejad, S., 2016. Control and treatment of sulfur compounds specially sulfur oxides (SO_x) emissions from the petroleum industry: A review. *Chem. Int.* 2, 242–253.
- Jafarinejad, S., 2017a. Activated sludge combined with powdered activated carbon (PACT process) for the petroleum industry wastewater treatment: A review. *Chem. Int.* 3, 368–377.
- Jafarinejad, S., 2017b. Recent developments in the application of sequencing batch reactor (SBR) technology for the petroleum industry wastewater treatment. *Chem. Int.* 3, 241.
- Jazie, A., Pramanik, H., Sinha, A., Jazie, A., 2013. Egg shell as eco-friendly catalyst for transesterification of rapeseed oil: optimization for biodiesel production. *Int. J. Sustain. Develop. Green Econom.* 2, 27–32.
- Jazie, A.A., Pramanik, H., Sinha, A., 2012. Egg Shell Waste-Catalyzed Transesterification of Mustard Oil: Optimization Using Response

- Surface Methodology (RSM). *Int. Proc. Comput. Sci. Inform. Technol.* 56, 52.
- Jiménez-Cruz, F., Marín-Rosas, C., Castañeda-Lopez, L.C., García-Gutiérrez, J.L., 2021. Promising extruded catalyst for palm oil transesterification from LiAlH₄ hydrolysates. *Arab. J. Chem.* 14 (5), 103141. <https://doi.org/10.1016/j.arabjc.2021.103141>.
- Joya, M., Bautista, J.B., Raba, A.M., 2016. Quicklime as an alternative in the photodegradation of contaminants. *Journal of Physics: Conference Series*. IOP Publishing 687, 012044. <https://doi.org/10.1088/1742-6596/687/1/012044>.
- Kesic, Z., Lukic, I., Zdujic, M., Mojovic, L., Skala, D., 2016. Calcium oxide based catalysts for biodiesel production: A review. *Chem. Ind. Chem. Eng. Quart.* 22 (4), 391–408.
- Kirubakaran, M., Selvan, V.A.M., 2021. Experimental investigation on the effects of micro eggshell and nano-eggshell catalysts on biodiesel optimization from waste chicken fat. *Bioresour. Technol. Report.* 14, 100658. <https://doi.org/10.1016/j.biteb.2021.100658>.
- Kostić, M.D., Bazargan, A., Stamenković, O.S., Veljković, V.B., McKay, G., 2016. Optimization and kinetics of sunflower oil methanolysis catalyzed by calcium oxide-based catalyst derived from palm kernel shell biochar. *Fuel* 163, 304–313.
- Kuniyil, M., Shanmukha Kumar, J.V., Adil, S.F., Assal, M.E., Shaik, M.R., Khan, M., Al-Warthan, A., Siddiqui, M.R.H., 2021. Production of biodiesel from waste cooking oil using ZnCuO/N-doped graphene nanocomposite as an efficient heterogeneous catalyst. *Arab. J. Chem.* 14 (3), 102982. <https://doi.org/10.1016/j.arabjc.2020.102982>.
- Lee, S.L., Wong, Y.C., Tan, Y.P., Yew, S.Y., 2015. Transesterification of palm oil to biodiesel by using waste obtuse horn shell-derived CaO catalyst. *Energy Convers. Manage.* 93, 282–288.
- Mardhiah, H.H., Ong, H.C., Masjuki, H., Lim, S., Lee, H., 2017. A review on latest developments and future prospects of heterogeneous catalyst in biodiesel production from non-edible oils. *Renew. Sustain. Energy Rev.* 67, 1225–1236.
- Mene, D.F., Iwuoha, G.N., 2021. Genotoxicity and carcinogenicity of traditionally roasted meat using indicator polycyclic aromatic hydrocarbons (PAHs), Port Harcourt, Nigeria. *Chem. Int.* 7, 217–223.
- Mohsin, M., Bhatti, I.A., Ashar, A., Mahmood, A., ul Hassan, Q., Iqbal, M., 2020. Fe/ZnO@ ceramic fabrication for the enhanced photocatalytic performance under solar light irradiation for dye degradation. *J. Mater. Res. Technol.* 9 (3), 4218–4229.
- Mootabadi, H., Salamatinia, B., Bhatia, S., Abdullah, A.Z., 2010. Ultrasonic-assisted biodiesel production process from palm oil using alkaline earth metal oxides as the heterogeneous catalysts. *Fuel* 89 (8), 1818–1825.
- Mumtaz, M., Adnan, A., Mukhtar, H., Rashid, U., Danish, M., 2017. Biodiesel Production Through Chemical and Biochemical Transesterification: Trends, Technicalities, and Future Perspectives. *Clean Energy for Sustainable Development*. Elsevier, 465–485.
- Nejad, A.S., Zahedi, A.R., 2018. Optimization of biodiesel production as a clean fuel for thermal power plants using renewable energy source. *Renew. Energy* 119, 365–374.
- Niju, S., Meera, K.M., Begum, S., Anantharaman, N., 2014. Modification of egg shell and its application in biodiesel production. *J. Saudi Chem. Soc.* 18 (5), 702–706.
- Nisar, N., Mehmood, S., Nisar, H., Jamil, S., Ahmad, Z., Ghani, N., Oladipo, A.A., Qadri, R.W., Latif, A.A., Ahmad, S.R., Iqbal, M., Abbas, M., 2018. Brassicaceae family oil methyl esters blended with ultra-low sulphur diesel fuel (ULSD): Comparison of fuel properties with fuel standards. *Renew. Energy* 117, 393–403.
- Obi, C., Ibezim-Ezeani, M.U., Nwagbo, E.J., 2020. Production of biodiesel using novel *C. lepodita* oil in the presence of heterogeneous solid catalyst. *Chem. Int.* 6, 91–97.
- Okullo, A.A., Temu, A., Ogowok, P., Ntalikwa, J., 2012. Physico-chemical properties of biodiesel from jatropha and castor oils. *Int. J. Renew. Energy Res.* 2, 47–52.
- Onukwuli, D.O., Emembolu, L.N., Ude, C.N., Aliozo, S.O., Menkiti, M.C., 2017. Optimization of biodiesel production from refined cotton seed oil and its characterization. *Egypt. J. Petrol.* 26 (1), 103–110.
- Oyerinde, A., Bello, E., 2016. Use of fourier transformation infrared (FTIR) spectroscopy for analysis of functional groups in peanut oil biodiesel and its blends. *Curr. J. Appl. Sci. Technol.* 13 (3), 1–14.
- Pedavaoh, M.-M., Badu, M., Boadi, N.O., Awudza, J.A., 2018. Green Bio-Based CaO from Guinea Fowl Eggshells. *Green Sustain. Chem.* 8, 208.
- Popovicheva, O.B., Irimiea, C., Carpentier, Y., Ortega, I.K., Kireeva, E.D., Shonija, N.K., Schwarz, J., Vojtišek-Lom, M., Focsa, C., 2017. Chemical composition of diesel/biodiesel particulate exhaust by FTIR spectroscopy and mass spectrometry: impact of fuel and driving cycle. *Aerosol Air Qual. Res.* 17 (7), 1717–1734.
- Puna, J.F., Gomes, J.F., Correia, M.J.N., Soares Dias, A.P., Bordado, J.C., 2010. Advances on the development of novel heterogeneous catalysts for transesterification of triglycerides in biodiesel. *Fuel* 89 (11), 3602–3606.
- Ramos, M., Dias, A.P.S., Puna, J.F., Gomes, J., Bordado, J.C., 2019. Biodiesel production processes and sustainable raw materials. *Energies* 12, 4408.
- Ranganathan, L., Sampath, S., 2011. A review on biodiesel production, combustion, emissions and performance. *Int. J. Adv. Sci. Tech. Res.* 13, 1628–1634.
- Saifuddin, N., Refal, H., 2014. Spectroscopic analysis of structural transformation in biodiesel degradation. *J. Appl. Sci. Eng. Technol.* 8, 1149–1159.
- Sasmaz, Ahmet, 2020. The Atbara porphyry gold–copper systems in the Red Sea Hills, Neoproterozoic Arabian-Nubian Shield. *NE Sudan. J. Geochem. Explor.* 214, 106539. <https://doi.org/10.1016/j.gexplo.2020.106539>.
- Shammout, M.W., Awwad, A.M., 2021. A novel route for the synthesis of copper oxide nanoparticles using Bougainvillea plant flowers extract and antifungal activity evaluation. *Chem. Int.* 7, 71–78.
- Sharma, S., Rangaiah, G.P., 2013. Multi-objective optimization of a bio-diesel production process. *Fuel* 103, 269–277.
- Sinanoglu, D., Sasmaz, A., 2019. Geochemical evidence on the depositional environment of Nummulites accumulations around Elazığ, Sivas, and Eskişehir (Turkey) in the middle Eocene subepoch. *Arab. J. Geosci.* 12, 759.
- Sivaramakrishnan, K., Ravikumar, P., 2012. Determination of cetane number of biodiesel and its influence on physical properties. *J. Eng. Appl. Sci.* 7, 205–211.
- Song, L., Zhang, S., 2010. Preparation and visible light photocatalytic activity of Bi₂O₃/CaO photocatalysts. *React. Kinet. Mech. Catal.* 99, 235–241.
- Tamborini, L.H., Militello, M.P., Balach, J., Moyano, J.M., Barbero, C.A., Acevedo, D.F., 2019. Application of sulfonated nanoporous carbons as acid catalysts for Fischer esterification reactions. *Arab. J. Chem.* 12 (8), 3172–3182.
- Thanh, L.T., Okitsu, K., Boi, L.V., Maeda, Y., 2012. Catalytic technologies for biodiesel fuel production and utilization of glycerol: a review. *Catalysts* 2 (1), 191–222.
- Tsegaye, M., Chandravanshi, B.S., Feleke, S., Redi-Abshiro, M., 2021. Enhanced cellulose efficiency of pressurized hot water pretreated highland Ethiopian bamboo (*Yushania alpina*): A potential feedstock for ethanol production. *Chem. Int.* 7, 53–61.
- Zhang, H., Ran, X., Wu, X., Zhang, D., 2011. Evaluation of electro-oxidation of biologically treated landfill leachate using response surface methodology. *J. Hazard. Mater.* 188 (1-3), 261–268.